


Giant ice rings on lakes and field observations of lens-like eddies in the Middle Baikal (2016–2017)

Alexei V. Kouraev ^{1,2*} Elena A. Zakharova,³ Frédérique Rémy,¹ Andrey G. Kostianoy,^{4,5} Mikhail N. Shimaraev,⁶ Nicholas M. J. Hall,¹ Roman E. Zdrovennov,⁷ Andrey Ya Suknev⁸

¹LEGOS, Université de Toulouse, CNES, CNRS, IRD, UPS, Toulouse, France

²Tomsk State University, Tomsk, Russia

³Institute of Water Problems, Russian Academy of Sciences, Moscow, Russia

⁴P.P. Shirshov Institute of Oceanology, Russian Academy of Sciences, Moscow, Russia

⁵S.Yu. Witte Moscow University, Moscow, Russia

⁶Limnological Institute, Siberian Branch of the Russian Academy of Sciences, Irkutsk, Russia

⁷Northern Water Problem Institute, Karelian Center of the Russian Academy of Sciences, Petrozavodsk, Russia

⁸Great Baikal Trail (GBT) Buryatiya, Ulan-Ude, Russia

Abstract

Giant ice rings (diameter 5–7 km) detected on lakes Baikal (Russia) and Hovsgol (Mongolia) are a surface manifestation of intrathermocline lens-like eddies under ice cover. By analyzing satellite imagery, we have detected new ice rings in 2016 and very old ones in 1969 for Lake Baikal. We have also discovered a giant ice ring on a new water body—Lake Teletskoye in the Altai Republic (Russia). Our recent field observations in the Middle Baikal have high temporal and spatial resolution and coverage and include temperature and current measurements over a long (1.5 month) period. In 2016, an eddy was detected in February and then an eddy and ice ring were detected in March at the same location. In 2017, another eddy was detected in February. This eddy was not stationary, as it was detected 6 km from its initial position in March, and thus no ice ring formed. The results of our field observations provide new data on the size and shape of the eddies. Indirect and direct measurements of currents and temporal evolution of the temperature field make it possible to estimate the rotation period (3 d) for the eddy in 2016 and assess the timing of movement, position, and displacement speed of the eddy in 2017. Thermal infrared Landsat imagery before ice formation in November–December 2015 shows that the eddy in 2016 was formed by the wind-induced outflow from the Barguzin bay.

Giant ice rings were first observed on satellite images in Lake Baikal, Russia (Granin et al. 2005, 2008). They are rings of dark (thinner) ice with white (thicker) ice in the center and outside of the ring. The rings have a typical diameter of 5–7 km and a width of 0.9–1.3 km. Due to the size of the ice rings their detection is possible only from satellite images. The rings appear in different places in Lake Baikal and in different years in a seemingly unpredictable manner. Their circular form, large size, and unclear origins have sparked scientific and public interest.

In our previous work (Kouraev et al. 2016), we made an attempt to better understand the ice rings phenomenon. Based

on archives of satellite imagery and photography for 1974–2014, we made the most complete existing inventory of the ice rings with 45 rings identified for Lake Baikal and also for the first time four rings for the neighboring Lake Hovsgol (Mongolia).

To improve our understanding of the phenomena leading to the formation, development, and disappearance of ice rings, we carry out dedicated field measurements in the regions where ice rings appear. In the framework of French–Russian–Mongolian cooperation every spring (March–April) we conduct field observations of ice cover and associated water structure in the central part of Lake Baikal (since 2010) and in Lake Hovsgol (since 2014). The existing data set (as of 2017) contains data from more than 380 stations in regions of known ice ring observations and along satellite tracks of radar altimetry missions (Kouraev et al., 2015).

Our hydrographic surveys beneath the ice rings in Lake Baikal in 2012–2014 and in Lake Hovsgol in 2015 have shown the presence of warm lens-like (double-convex form) eddies

*Correspondence: kouraev@legos.obs-mip.fr

This is an open access article under the terms of the Creative Commons Attribution-NonCommercial-NoDerivs License, which permits use and distribution in any medium, provided the original work is properly cited, the use is non-commercial and no modifications or adaptations are made.

before and during the manifestation of ice rings (Kouraev et al. 2016). We have shown that giant ice rings are a surface manifestation of these intrathermocline lens-like eddies. These eddies exist before and during the manifestation of the ice rings. They have an isolated circular form and radial symmetry, and their position corresponds to the location of ice rings.

Lens-like eddies are known to exist in the ocean (Dugan et al. 1982; Armi and Zenk 1984; McWilliams 1985; Kostianoy and Belkin 1989; Richardson et al. 2000), but only a few observations exist for lakes (Forrest et al. 2013; Granin et al. 2015, 2018; Graves 2015; Kirillin et al. 2015; Kouraev et al. 2016, 2018a). Moreover, these works provide a mostly “static” image of the eddies with some analysis of temporal evolution over just several days or at best repeat profiles done after ice breakup (Granin et al. 2018).

At the same time, very little is known about the mesoscale and submesoscale circulation in Lake Baikal even during the ice-free period. Numerical modeling (LeCore 1998; Tsvetova 1999; Lawrence et al. 2002) reproduces the cyclonic gyres at the scale of the three sub-basins of the lake quite well, but generally does not reveal smaller eddy-like structures. Various satellite remote sensing techniques have been used to assess the spatial distribution of surface properties and analyze water dynamics (LeCore 1998; Semovski et al. 2000b; Heim et al. 2005; Troitskaya et al. 2015), but in most cases present only isolated examples of potential of remote sensing applications.

Despite recent advances regarding lens-like eddies in lakes Baikal and Hovsgol in winter several open questions remain. What is their motion under ice? Are they stationary or moving? Are they formed before or after ice formation and how long do they last? What are the mechanisms of eddy generation and development? To address these questions, we continue to analyze satellite imagery to update the inventory of ice rings as surface manifestation of lens-like eddies, and we continue to perform in situ measurements of lens-like eddies in Lake Baikal yearly.

However the main goal of the work presented here is to analyze new in situ data for 2016 and 2017 in order to better assess their parameters (location, shape, internal structure, current speed, direction of rotation) and assess further characteristics (timing, stationarity or not) that may help to understand the mechanisms responsible for eddy generation. Our field work is aimed to get much longer coverage of water dynamics in the regions of the eddies and surrounding regions. To do this, we have modified our field survey strategy for the Middle Baikal by improving temporal and spatial resolution (see Methods section). In 2016, an eddy was detected in February and then, an eddy and ice ring were detected in March at the same location. In 2017, an eddy was detected in February, which then moved but was detected 6 km from its initial position in March, and no ice ring formed. We discuss the implications of our results for better understanding eddy dynamics and address several of the questions raised above.

Study site

Lake Baikal is the deepest lake in the world. Its bottom is separated into three parts: deep depressions in the southern and middle parts (maximum depths 1461 and 1642 m, correspondingly), and a shallower depression (maximum depth 904 m) in the northern part. Despite the large volume of the lake and associated thermal inertia, long and cold winters result every year in a complete freeze-up of the lake surface for 5–6 months between December–January and April–May (Verbolov et al. 1965; Galaziy 1993; Kouraev et al., 2007 *a,b*). The presence and state of ice cover is important for the hydrophysical structure, spring bloom of diatoms and primary productivity (Granin et al. 1999; Semovski et al. 2000a; Mackay et al. 2003, 2005; Moore et al. 2009), as well as for the living conditions of the endemic Baikal seal (*Pusa sibirica*, *Phoca sibirica*). The presence of ice is also crucial for establishing transport for fishing activities and tourism.

Our field work takes place in the region of the Nizhneye Izgolovye Cape in the Middle Baikal, where the head of the underwater depression (depth 1000–1500 m) is located between the Akademicheskii Ridge and Svyatoy Nos Peninsula (Fig. 1). This is the region where we often observe giant ice rings and where we detected lens-like eddies in 2012 and 2014 (Kouraev et al. 2016).

Methods

Ice rings detection

We have processed and visually analyzed optical and infrared satellite imagery from Terra and Aqua (MODIS sensor), Landsat and declassified Corona (KeyHole-4a, mission 1051-2) satellites. For more details on ice rings detection methodology please see Kouraev et al. (2016).

In situ monitoring strategy

Our previous field studies provided mostly a “snapshot” of the spatial distribution of ice cover and the water structure in the middle of winter. To fully understand the evolution of water structure and dynamics, there is a need to have better temporal resolution and larger time span. Starting from 2016, we have changed our monitoring strategy—every winter we carry out not one, but two field surveys that take place in mid-February and (as usual) in late March. During each survey we perform (1) surface measurements of ice thickness and snow depth, as well as ice structure and roughness, (2) vertical profiles of temperature and conductivity, and (3) direct and indirect estimation of current field. We also install temperature loggers and current meters that stay in place between the February and March.

CTD casts

Since 2012, parameters of the water column were measured using the CastAway (SonTek, USA) CTD (conductivity, temperature, depth) probe—accuracy 0.05°C, resolution 0.01°C, conductivity—accuracy $0.25\% \pm 5 \mu\text{S cm}^{-1}$, resolution $1 \mu\text{S cm}^{-1}$). Conductivity has been recalculated to specific conductance at

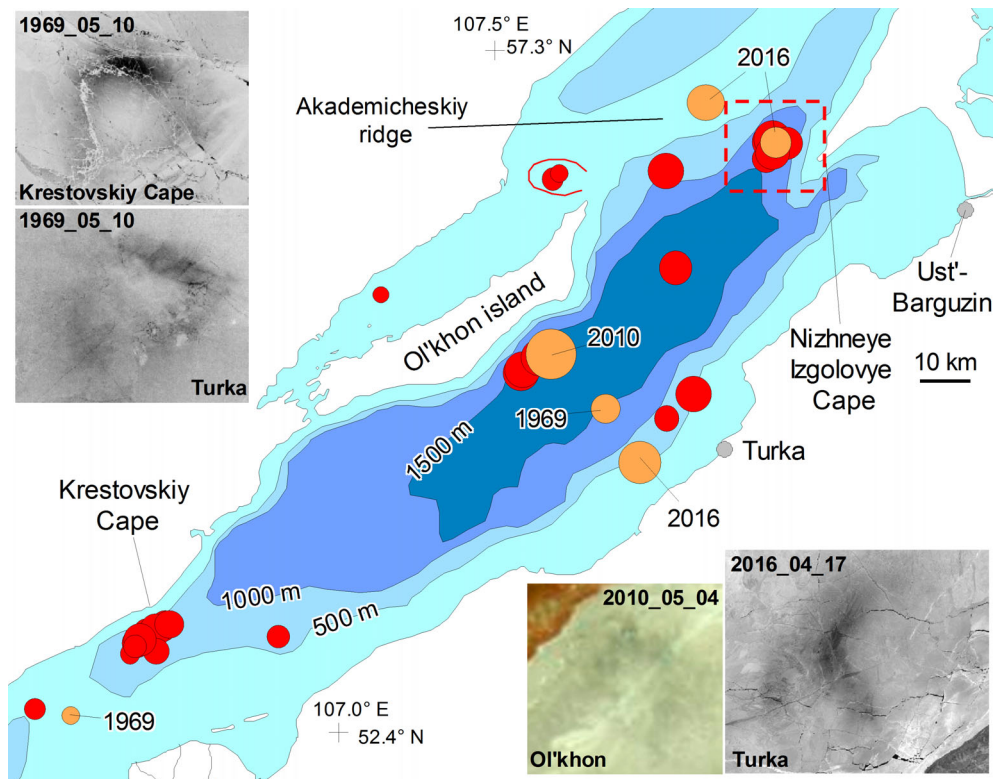


Fig. 1. Overview map of the Middle Baikal and region of field work (red dashed rectangle). Also shown are previously detected (red circles) and newly detected (orange circles) ice rings as well as their satellite images (1969—Corona, 2010—MODIS, 2016—Landsat).

0 dbar pressure and 3.5°C (Blinov et al. 2006). However, this CTD operates only down to 100-m depth. To get information on deeper layers, since 2016 we also use RBR (Canada) Solo T temperature logger (accuracy $\pm 0.002^\circ\text{C}$, resolution $< 0.0005^\circ\text{C}$) and TD Duet temperature/depth logger (2 Hz sampling, temperature accuracy $\pm 0.002^\circ\text{C}$, resolution $< 0.0005^\circ\text{C}$, pressure accuracy 0.85 m, and resolution 1.7 cm). These temperature measurements were made down to 160 m (February 2016) and to about 200 m (all other surveys).

Currents

Previously currents were estimated only semiquantitatively by measuring direction and current strength (weak, moderate, or strong) from CTD cable inclination. While current direction is a quantitative measurement, current strength is estimated by a visual expert assessment and is only qualitative. Now we complement these measurements by (1) passive drifters to estimate currents just under the ice (similar semi-quantitative approach as described before), (2) a SeaHorse (USA) tilt current meter—one version without compass (only current speed) and one SH1p70M with 3-axis accelerometer (0.002 g accuracy) with compass (current speed and direction), and (3) during the survey in March 2017—a Compact EM (Alec Electronics, Japan) miniature electromagnetic current recorder (current

velocity: accuracy $\pm 1 \text{ cm s}^{-1}$, resolution 0.02 cm s^{-1} ; direction: accuracy $\pm 2^\circ$, resolution 0.01°).

Long-term loggers

Basing on the February results, we identified the position of the eddy and installed several 100-m long ropes (anchored in the ice and weighted at the bottom) with RBR Solo T temperature sensors and SeaHorse tilt current meters. Each SeaHorse was attached to the main rope with a secondary 10-cm long rope and had thus a stable position in the water column. In 2016, we installed two ropes—one inside and another outside of the eddy. On each rope were installed RBR Solo T loggers (at depths 5, 25, 45, 65, and 85 m, time step 10 min) and SeaHorse current meters (at 45 m depth, time step 5 min). In 2017, we installed three ropes—one inside the eddy, another outside the eddy boundary, and third in the background conditions. Ropes 1 and 2 had RDR Solo loggers at depths 5, 25, 45, 65, and 85 m, and rope 3 had them at depths 5, 45, and 85 m. Also on ropes 1 and 3, SeaHorse current meters were installed at 45-m depth, with a compass on rope 1.

These ropes stayed in place until the next mission in March, providing continuous observations between mid-February and the end of March and helping to estimate temporal and spatial changes in water structure and dynamics for

Table 1. Inventory of newly detected ice rings and their characteristics. For the method used to define ice rings and the previous inventory see Kouraev et al. (2016).

Year (end of winter)	Name	Diameter, km	Lon E	Lat N	First seen*	Last seen*	Duration, days [†]	Depth, m	Form [‡]
1969	Turka	6	107.85	53.02	05/10	05/10	(1)	1350	ODR
1969	Krestovskiy C. SW	4	106.15	52.43	05/10	05/10	(1)	450	OR
2010	Olkhon east	10.6	107.68	53.12	05/04 (4)	05/18 (3)	15	1550	R
2010	Teletskoye Lake	3.2	87.74	51.46	04/12	04/12	(1)	275	OR
2016	N. Izgolovye C.	6.6	108.39	53.53	03/16 (1)	04/20 (1)	36	1400	R
2016	N. Izgolovye C. No2	7.6	108.17	53.60	04/13 (2)	04/20 (1)	8	450	OR
2016	Turka	9	107.95	52.92	04/15 (4)	04/23 (1)	9	650	OR

C., Cape; N. Izgolovye, Nizhneye Izgolovye; SW, southwest.

*Date format is (MM/DD); numbers in brackets—Days since last ring-free scene for first ring seen, and days to first ring-free scene after last ring observation.

[†]Duration is defined as difference between the first observation and the last one. For observations based on non-MODIS imagery, duration is put in brackets, meaning “at least X days,” though ring could have existed longer.

[‡]Form of the ring (influenced by ice structure and snow cover). R, ring; OR, open ring (not completely closed); ODR, open diamond ring (open ring with a large dark patch).

1.5 months. To our knowledge, so far there are no comparable long-term observations of eddies under lake ice.

Results

New ice rings detected

By analyzing satellite imagery, we have been able to detect several new ice rings (Table 1, see also Fig. 1). While our previous detection of ice rings using Landsat imagery showed the presence of ice rings as early as 1974 (Lake Baikal) and 1975 (Lake Hovsgol), Corona imagery brings even earlier detection—1969, when two ice rings near Turka and near Cape Krestovskiy were simultaneously observed on 10 May. This again confirms our previous conclusion that although recently documented, ice rings are not a recent phenomenon.

We have also detected a new ice ring near Olkhon Island in 2010, and three more rings in 2016. No ice rings have been observed in 2017 for Lake Baikal and no new ice rings for Lake Hovsgol. However, we have also discovered ice rings in a new water body—Lake Teletskoye (Kouraev et al. 2018*b, c, d*; Leech 2018).

Lake Teletskoye is located about 1000 km west from Lake Baikal, in the Altai Republic, not far from the Mongolian border. The lake has a long (78 km) and narrow (average width 2.9 km) shape, with steep bathymetry and maximum depths up to 323 m (Mitrofanova and Kirillov 2012). While lakes Baikal and Hovsgol freeze every year for several months, Lake Teletskoye is fully ice covered only in some years. In 2010, when stable ice cover formed on the whole lake, an ice ring was detected in April in the southern part of the lake, over depths up to 275 m, in the head of an underwater depression. The ring was small (3.2 km diameter, limited by the lake width), but well-defined.

Previously detected ice rings in Lake Hovsgol (Kouraev et al. 2016) and now for Lake Teletskoye also confirm our previous conclusions that ice rings (and associated underwater eddies) are a phenomenon that is not limited to Lake Baikal.

Field survey in February 2016

Stable ice cover in the region of the Nizhneye Izgolovye Cape formed on 22 January 2016. 20 d later during our field observations (12–14 February 2016), we detected anomalies in water structure (temperature and specific conductivity) indicating the presence of a lens-like eddy, which typically leads to the formation of the giant ice rings. We performed a detailed survey with high spatial resolution of the region with this anomaly (Fig. 2).

Vertical profiles of temperature (Fig. 3) show the presence of a well-developed lens-like eddy that has a double-convex form. The vertical center of the eddy is located at the 45-m depth, which is similar to our previous observations in this region in 2012 and 2014 (Kouraev et al. 2016). The core of the eddy has uniform temperature values: 1–1.4°C in the upper 0–45 m part; which is warmer than the surrounding regions (0.3–0.6°C) and 1.4–2.2°C in the lower 45–160 m part, which is colder than temperature outside (2.6–3.5°C). Use of the RBR Solo T logger shows that the downward inclination of isotherms in the lower part of the eddy extends well below 160 m.

Using our observations, we are able to determine the spatial distribution of depth at which specific isotherms are positioned (Fig. 4). We have selected isotherms at 1.2°C, which rises almost to the lower ice cover boundary and 1.65°C, which goes almost to the 100-m depth (the lowest depth of observations for most stations). The 1.2°C isotherm is located at a depth 35–40 m outside the eddy, and within the eddy it rises sharply to 2–5-m depth forming a flat dome in the central part. The 1.65°C isotherm is located at 35–50 m outside

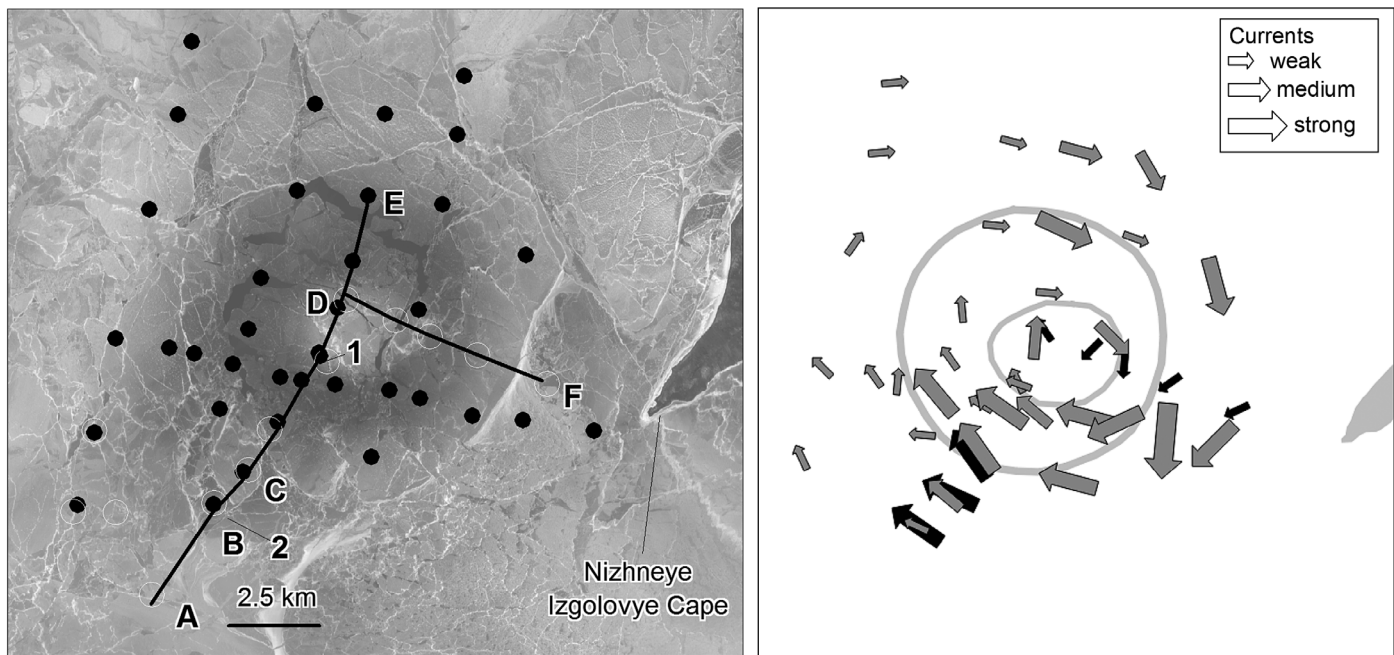


Fig. 2. Left panel: Map of stations for 12–14 February 2016 (black circles) and 28–30 March 2016 (open white circles), location of ropes with thermistors (1 and 2) and transects across the eddy. Background—Landsat 8 image from 01 April 2016. Right panel: Current direction and strength (weak–medium–strong, measured by CTD cable inclination and denoted by arrow size) for February (gray arrows) and March (black arrows). Gray circles—Location of the giant ice ring as defined from Landsat 8 image from 01 April 2016 (see left panel).

the eddy, and plunges down to 90–95-m depth in the central part where it forms a large plateau with some local depressions. The temperature distribution within the eddy has mostly radial symmetry but with some irregularities. Another interesting feature is that while both upper and lower parts of the eddy are well collocated, the spatial extent of the rising in the upper part of the eddy (that corresponds very well to the position of the future ice ring) is smaller than that of the downward inclination of isotherms in its lower part. This is explained by the fact that for the upper part of the eddy the water outside is homogeneous (after the autumnal overturning and consequent mixing down to 45-m depth), so the eddy extends laterally replacing the surrounding water. For the lower part of the eddy, the water outside of it is well stratified, the eddy is located within the inclined isothermal surfaces over a larger area.

The direction and strength of the currents (see Fig. 2) confirms the anticyclonic (clockwise) direction of rotation, which is a characteristic feature of lens-like (double-convex form) eddies, and is also in agreement with our previous findings for eddies in lakes Baikal and Hovsgol (Kouraev et al. 2016). The ice thickness distribution (not shown) indicates that the ice was thinner in the region of the center of the eddy and the future ice ring (45–48 cm) and north of it. Maximum ice thickness (60–65 cm) was found west of the eddy. The ice was black and crystalline and without impurities. No water was observed on the ice and no gas bubbles were present in the water under the ice.

Giant ice ring development in March–April 2016

The first ice ring appeared on satellite images unusually early—on 14 March (Fig. 5), with an outer diameter of 6.6 km (ring width was 1.7 km). Two days later on 16 March, an UAZ off-road van going from the Olkhon Island to Ust-Barguzin (see Fig. 1) fell through the ice in the region of the ice ring (the driver and passengers were rescued). On 18 March 2016 at the eastern boundary of the ice ring, another UAZ vehicle broke through the ice, but fortunately got stuck (Fig. 5) and was recovered next day. By the beginning of April, the ice ring was dissected by numerous large cracks and leads. The location of the ice ring corresponds exactly with the location of the eddy identified in mid-February. As shown in Kouraev et al. (2016), currents are absent or weak in the center of the eddy and strongest at the eddy periphery, so current speed (and thus intense heat exchange between ice and water), rather than presence of warmer water in the ring center, is the main driver related to ice melting and subsequent appearance of an ice ring. By 07–09 April, drifting ice floes concentrated in the southern part of the ice ring, which was now a hole. Several large cracks extended from the ice ring in the northwest and southeast directions. In the region 17 km northwest of the ice ring, another ice ring formed on 13 April. These two rings were visible until 20 April, and on 21 April under the influence of the wind, thin ice drifted southwest and was compacted, and these ice rings were no longer visible. Ice breakup started on 25 April and by 04 May, the Middle Baikal was ice free.

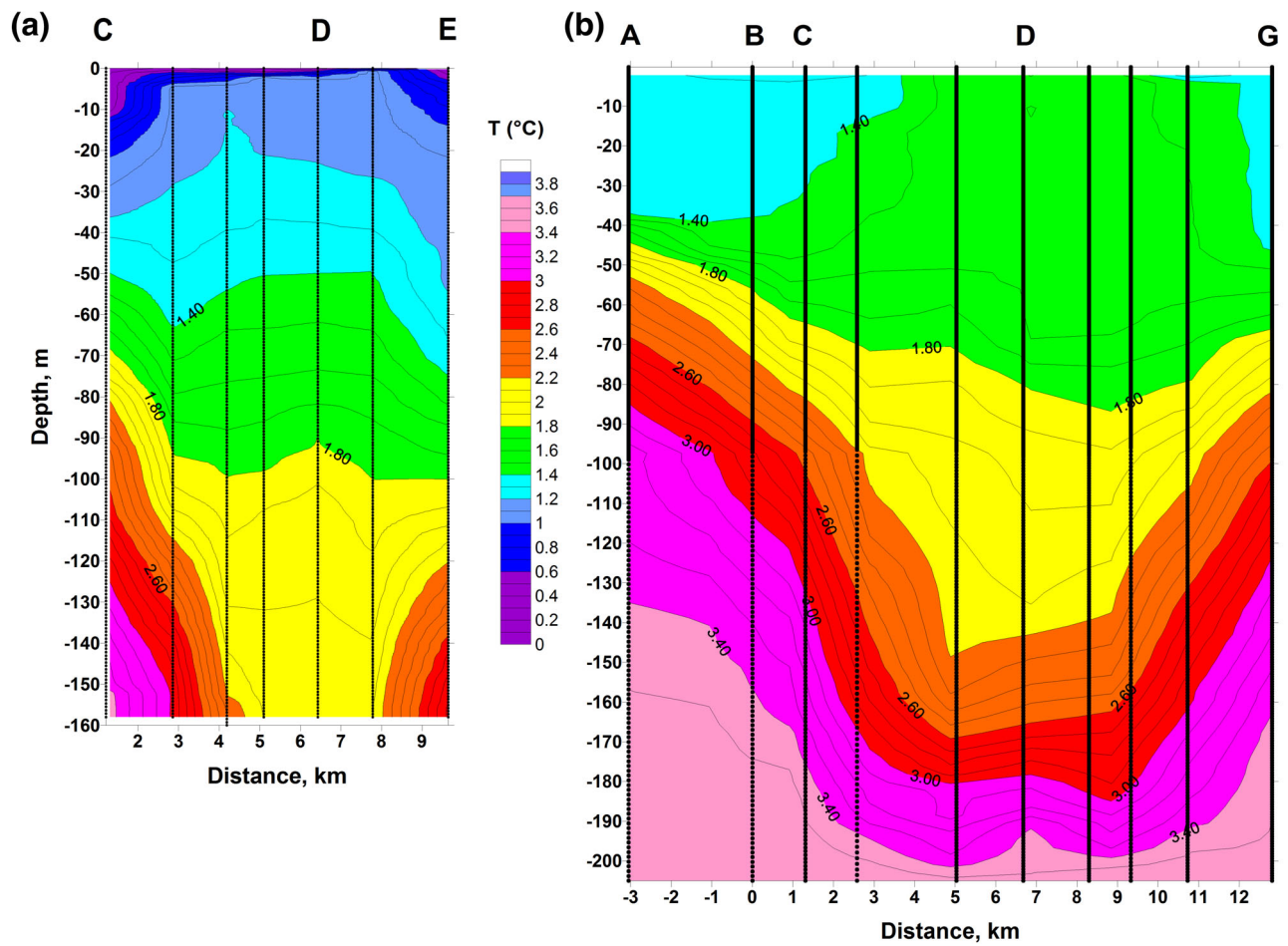


Fig. 3. Vertical sections of water temperature (°C) in (a) February 2016 and (b) March 2016. Vertical lines—station positions. For station locations see Fig. 2.

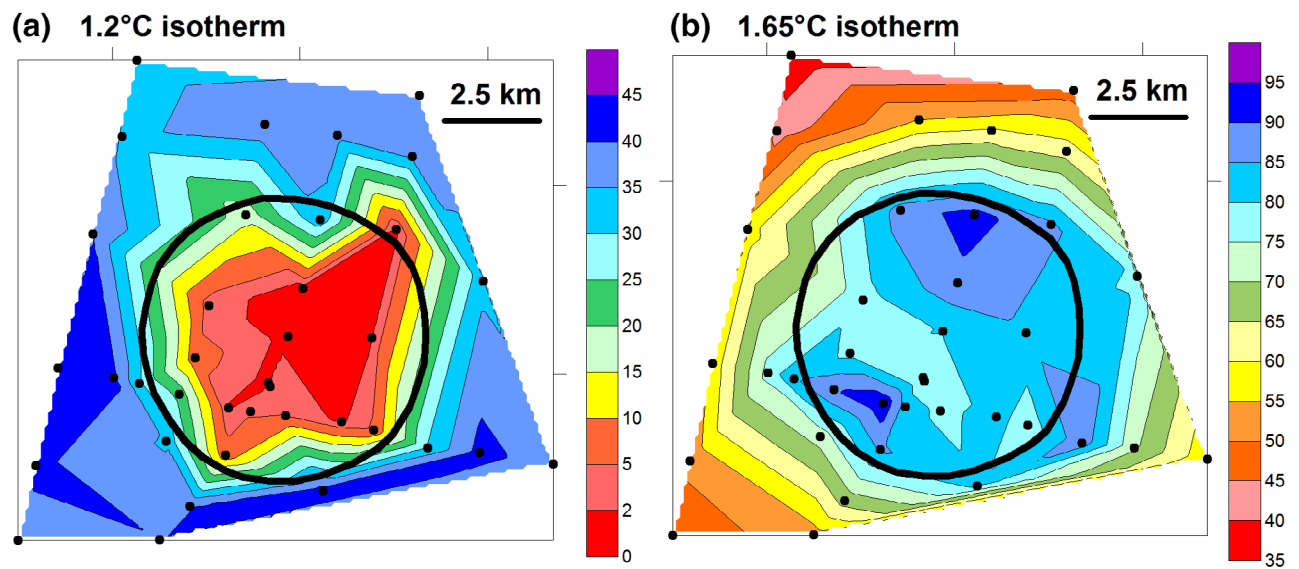


Fig. 4. February 2016. Depth (m) of isotherms 1.2°C (a) and 1.65°C (b). Black dots—Station locations, black circle—Outer boundary of the ice ring as defined on 01 April 2016.

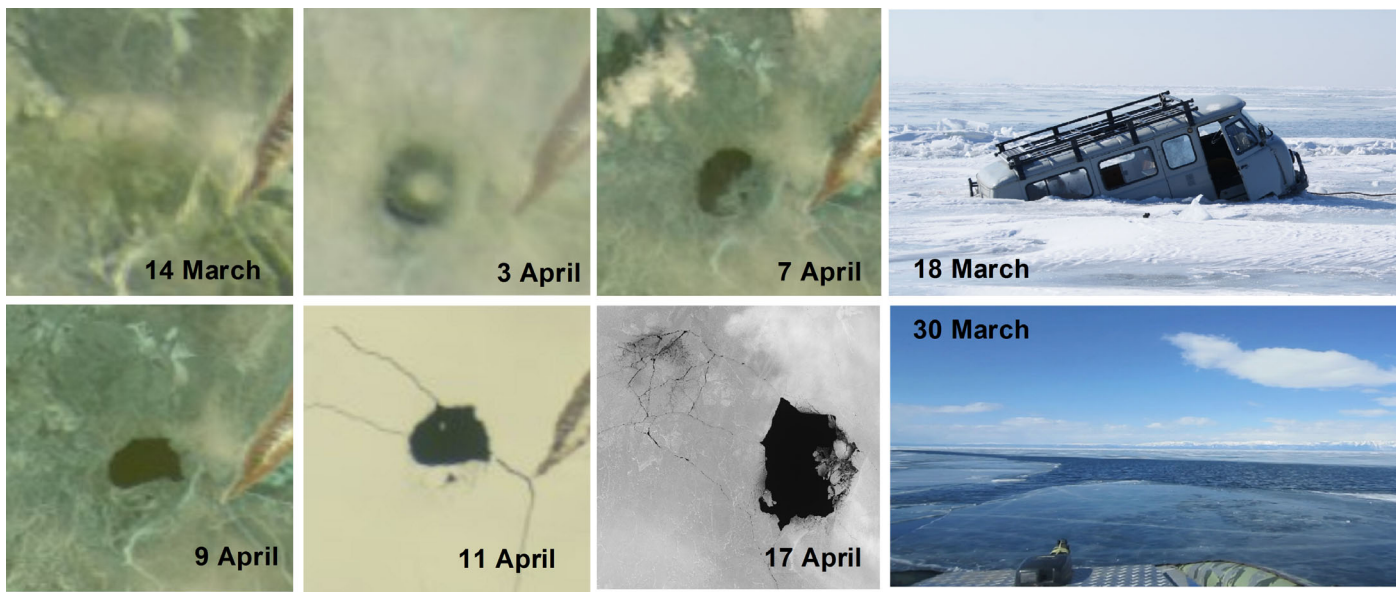


Fig. 5. Temporal evolution of the ice rings near the Cape Nizhneye Izgolye in 2016 from MODIS and Landsat 8 (17 April) imagery. Landsat image has a different scale to better illustrate the details. Right panel—UAZ vehicle trapped in ice on the eastern boundary of the ring on 18 March 2016 (photo by A. Beketov) and large leads (width 10 m and more) in the same region on 30 March 2016.

Extremely dangerous ice conditions in March 2016 show that apart from scientific interest in ice cover evolution and associated eddy dynamics, the presence of ice rings is a major concern for ensuring the safety of people traveling on ice (Kouraev et al. 2018*b,c,d*; Leech 2018). The difficulty of detecting weak ice in the ice rings, as compared to the much more common contraction of expansion cracks, and the unpredictability of their location from year to year underlines the need for better and timely communication on this natural phenomenon among nonscientists—fishermen, tourism agencies, tourists, journalists, local administration, and so on. We have created a dedicated bilingual web site (www.icerings.org) and a booklet where we explain the ice ring phenomenon and mechanisms of ice ring formation, provide monitoring of ice cover and ice ring location and suggest regions to avoid (potential ice ring formation), as well as propose modification of ice routes for transport.

Field survey in March 2016

Due to difficult ice conditions, we were not able to do as dense a network of stations as in February. Ice cover in the ring was covered by areas of thin ice, small and large holes, cracks and leads extending for several hundreds of meters. Profiles across the eddy (Fig. 3b, see Fig. 2 for station positions) show that its position had not changed, and the ice ring was formed in exactly the same place as the top of the eddy defined in February. The temperature profile shows that while in February the upper core of the eddy had a temperature of 1.2–1.4°C, now it was 1.4–1.6°C. In the lower part of the eddy, we also observe warming of water: while in February at

140–160 m, the temperature was 1.8–2.0°C, at the end of March, it was 2.4–2.6°C. Isotherms in the lower part had risen up, along with the core of the eddy. Temperature profiles in March were taken down to 210 m. Even at this depth, we observe isotherm inclination, although less pronounced.

The current direction shows the same anticyclonic rotation (see Fig. 2). Ice thickness measurements show that between mid-February and the end of March, outside the ice ring the ice became thicker by 10–14 cm in the southwestern corner, while in the ring region, we observe a loss of ice thickness by 14–18 cm. Actually, the loss was even greater than this, because inside the ring, ice thickness was measured for patches of stable ice cover where it was possible to make measurements, but in the neighboring regions, there were numerous holes, leads with open water or patches of extremely thin (a few-centimeter-thick) ice.

Data from loggers February–March 2016

The temporal evolution of temperature and current speed for the two ropes is presented in Fig. 6. For rope 2 outside the ice ring (15 February to 28 March), there is a gradual warming (from 0.2°C to 1.5°C) in the upper 5- to 40-m-deep layer, with more pronounced variability at depths 5–20 m. Below 40 m depth no trend is observed, but on some days, there are rapid changes in temperature. For deeper layers, there is some irregular variability in temperature, and by the end of the observation period (days 81–88), there are some oscillations with a period of about 1.5 d for the 70–85 m depths. Analysis of current speed and temperature variability at 45 m depth (Fig. 6b) shows that current speed varied between 8 and 12 cm s⁻¹ and the

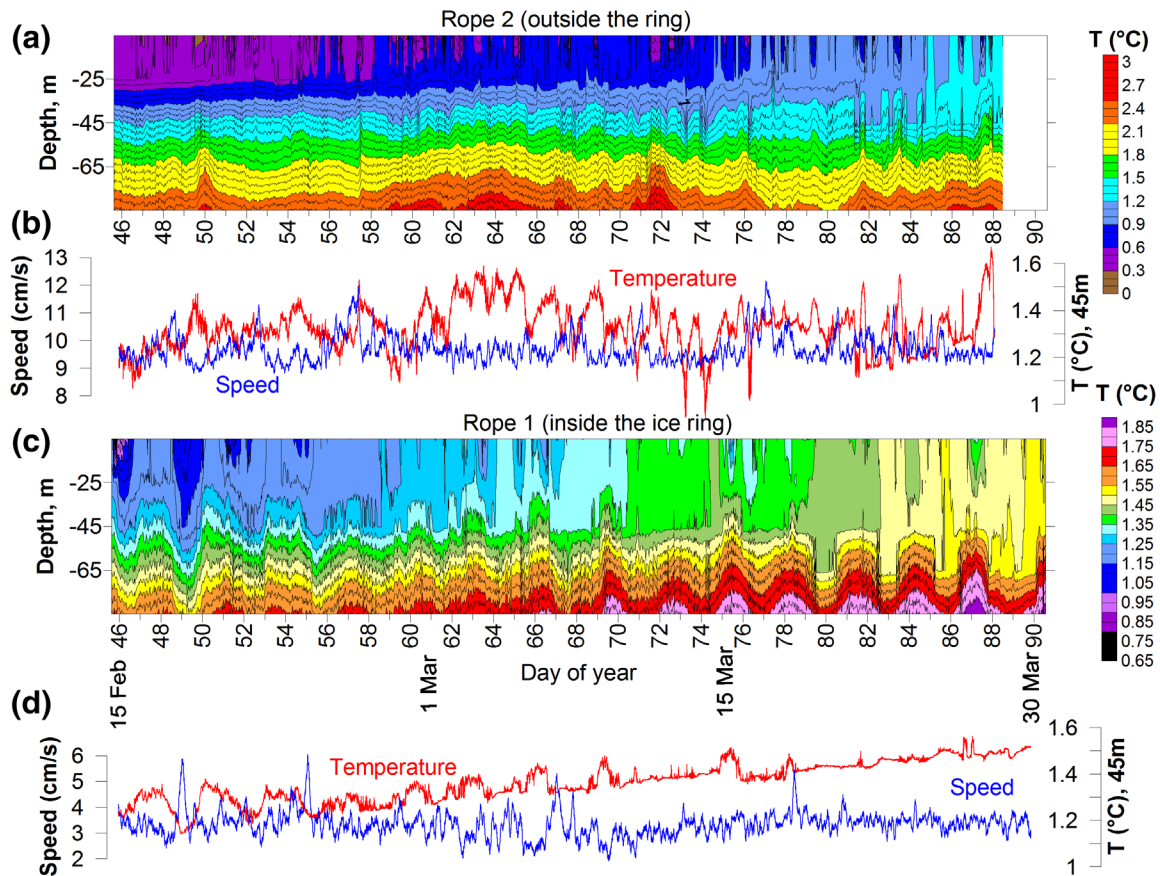


Fig. 6. Temporal evolution in February–March 2016 of the temperature profile (a), current speed and temperature at 45-m depth (b) for the rope outside the ice ring. (c) and (d) as (a, b), but for the rope inside the ice ring.

temperature varied between 1°C and 1.7°C . In many cases, rapid shifts in temperature and current speed are simultaneous. For several cases, there is a simultaneous decrease of speed and increase of temperature (days 49, 57, 71) or an increase of speed and decrease of temperature (days 67, 76). This shows the influence of lateral inflow from neighboring regions.

For rope 1 inside the ring (15 February to 30 March), the time series are very different (Fig. 6c,d). The upper part (5–25 m) shows gradual warming with much less temporal variability than in the same layer for the rope outside the ice ring. The temperature variability for the upper layer seems disconnected from deeper levels 35–85 m, where we observe regular vertical oscillations of isotherms. While in the beginning these oscillations affect water up to 25–35-m depth, by 10 May they affect water only at depths below 45 m (65 and 85 m) thus in the lower part of the eddy below the neutral level. Currents are much slower ($2\text{--}6\text{ cm s}^{-1}$) than outside the ice ring. The temperature at 45 m varies between 1.2°C and 1.6°C , with some oscillations mostly in the beginning up to day 55. Sharp increases in current speed are associated with decreases in temperature (days 49 and 55). Then a gradual warming trend is observed at a rate of $0.0087^{\circ}\text{C day}^{-1}$, in

some cases with overlaid oscillations, such as increase of temperature and decrease of speed at days 62, 65, 69, or increase of temperature and no significant changes in current speed at days 75 and 78. These overlaid oscillations at 45-m depth reflect temperature changes that happen at greater depths.

At the depths 65 and 85 m, we observe gradual warming of water with each oscillation, confirming rise of isotherms (eddy relaxation) in the lower part of the eddy (see also Fig. 4 and associated discussion). The period of temperature oscillations is about 3 d ($2.94\text{--}3.14\text{ d}$). A plausible explanation for these oscillations in the lower part of the eddy is that we observe the rotation of a not perfectly symmetrical eddy (see Fig. 4), which transports alternatively slightly warmer or colder water. As rope 1 was located 1.4 km from the eddy center, eddy rotation with a 3 d period gives a current speed of 3.39 cm s^{-1} which is in a perfect agreement with the average speed at 45-m depth (SeaHorse current meter) over the whole period of observations (3.35 cm s^{-1}). So temperature variability in the lower part of the eddy can be explained by a combination of (a) the rotation of a not perfectly symmetrical eddy and (b) the rise of isotherms in the lower part of the eddy and warmer water spreading to the upper part of the eddy core.

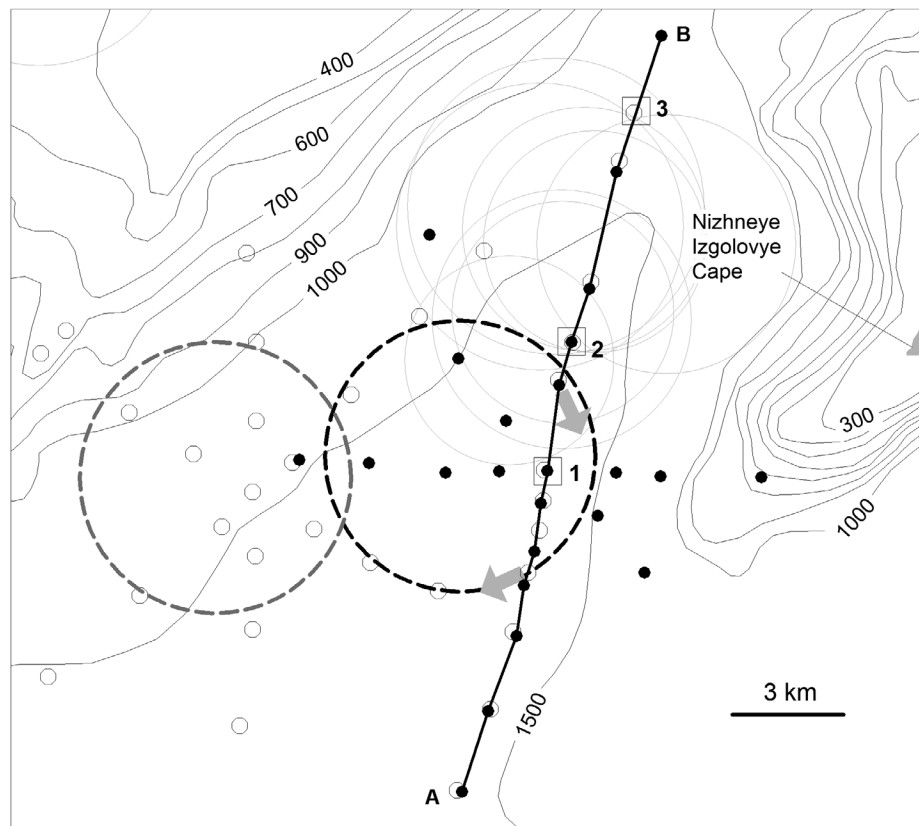


Fig. 7. Region of the Nizhneye Izgolovye Cape and bathymetry. Stations in February 2017 are shown as black circles, in March as open circles. Gray circles show the location of ice rings in previous years. Thick dashed circles show the possible location of the eddy (assuming 7-km diameter) in February (black) and March (gray). Black line shows the transect A-B. Black rectangles and numbers show the location of the three ropes. Gray arrows—Current direction measured by Alec current meters for 16–17 March 2017.

Field survey in February 2017

The first drifting ice appeared in the Middle Baikal on 10 January, and by 18 January, ice cover was stable. On 15–17 February, we detected from anomalies of water structure another lens-like eddy and did several transects. Based on the results obtained, we identified the potential position of the eddy (approximate diameter—7 km) and installed three ropes: rope 1 inside, rope 2 on the periphery of the eddy, and rope 3 in the head of the underwater canyon to monitor background conditions (Fig. 7).

As with our previous observations in the region of Cape Nizhneye Izgolovye in 2012, 2014 (Kouraev et al. 2016), and in 2016, we observe a well-developed warm lens-like eddy with similar characteristics as before. The eddy is as usual located at 45-m depth. The eddy in its upper part (0–45 m) is warmer ($0.6\text{--}1^{\circ}\text{C}$) than the surrounding regions ($0\text{--}0.2^{\circ}\text{C}$) and in its lower part is colder by about $0.8\text{--}1^{\circ}\text{C}$. By using the RBR Duet logger down to 200-m depth, we observe that the downward inclination of isotherms extends even further than 200 m (Fig. 8).

The distribution of current field speed and direction from semiquantitative approach again shows anticyclonic rotation. Direct measurements for 16–17 February 2017 of currents at

depth 45 m at two stations within the eddy by Alec current meters (see Fig. 7) show currents well aligned with the eddy shape. The current speed is similar ($3\text{--}4.4\text{ cm s}^{-1}$) for both Alec instruments that are located at the same distance from eddy center. The ice thickness varied between 50–60 cm in the northern part of the work area and 60–70 cm in the southern part. No specific ice thickness anomalies related to the eddy have been found.

Field survey in March 2017

Field work was conducted from 28 to 30 March (see Fig. 7 for station locations). On the first day, we repeated measurements along the transect A-B where we previously discovered the eddy. But the vertical structure indicates that the eddy was no longer present (Fig. 8b). The inclination of isotherms below 45 m was still present, but they had moved up. The layer with isotherms $0.6\text{--}1^{\circ}\text{C}$ did not change much—35–50 m in February vs. 35–45 m in March, but for example the 2.6°C isotherm rose by 65 m: 165-m depth in February vs. 100 m in March. However, in the upper part (0–45 m), there was no sign of the eddy. Instead there is homogeneous water with temperature $0.2\text{--}0.6^{\circ}\text{C}$.

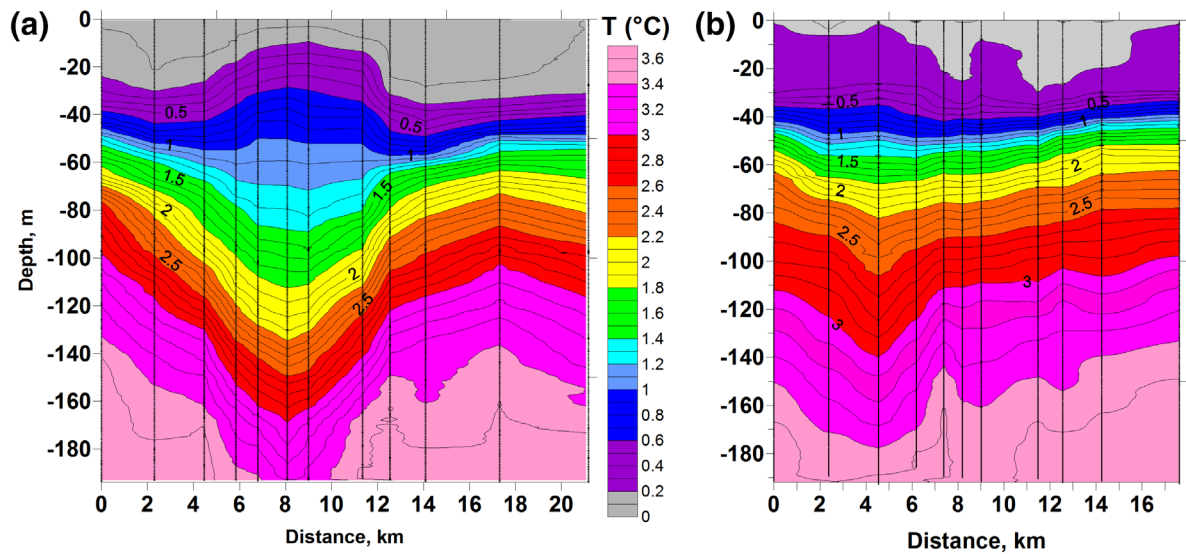


Fig. 8. Vertical sections of water temperature along transects A-B in February (a) and March (b) 2017. Vertical lines show station positions. For station locations see Fig. 7.

The eddy was eventually found at a new location about 6 km from its previous position. While there were some changes in absolute values of temperature, the shape and the size of the eddy were remarkably similar to February conditions, suggesting that this is the same eddy at a new position. So between 17 February and 28 March, the eddy moved from its location above the central part of the head of the underwater depression with more than 1500-m depth to a new location 6 km from its initial position above the slope with bathymetry changing from 900 to 1500 m (see Fig. 7).

Currents again confirm anticyclonic rotation of the eddy. The current field just below the ice and for the water column at 10–100-m depth shows stronger currents within the eddy and weak or no currents outside. The ice thickness distribution has not yet been affected by the eddy. Spatial differences are mostly related to snow cover depth. On the stations where there are ice thickness measurements for both February and March, ice generally got thicker by 20–30 cm.

Data from loggers February–March 2017

The three ropes installed in February (see Fig. 7) make it possible to monitor the temporal evolution of water temperature at different depths, as well as current speed and direction between mid-February and the end of March inside and outside the eddy (Fig. 9). Measurements with the Alec current meter in the region of the eddy for 16–17 February show currents with speeds of 3–4.4 cm s⁻¹ and direction 208° at 45 -m depth. The SeaHorse current meter installed at the same depth shows similar variability of current speed (3–4.5 cm s⁻¹) and current direction (160–200°) at the beginning of the measurements.

Thermistors installed on rope 1 show several periods with temperature variations. The first period (days 49–57, 18–26 February) shows a gradual decrease of vertical spread between

the isotherms. In the 0.3–0.6°C (violet) layer, the thickness did not change significantly (from 16 to 11 m) but its position (upper boundary) lowered from 15 to 27-m depth. The 0.6–0.9°C (blue) layer thinned from 15 to 11 m and lowered from 31 to 38 m. The 0.9–1.2°C (gray-blue) layer reduced in thickness from 21 to 12 m and slightly lowered from 46 to 49 m, while the 1.2–1.4°C (light-blue) layer thickness changed from 18 to 9 m and its position raised from 67 to 61 m. So we observe a convergence of layers toward a depth of about 55 m, with a decrease in layer thickness by 25–30% in the upper part and by 42–50% in the lower part of the eddy. This shows that the eddy was slowly leaving this area, probably in the north-west direction as we observe a clockwise change of current direction from 160 to 200°.

Starting from days 57 to day 67 (26 February to 08 March), we observe three examples of an increase and subsequent decrease of vertical distance between isotherms, as if the eddy was either vertically oscillating or making horizontal back and forth movements. This period is also characterized by a sharp increase in variability of current direction. After day 67, we observe gradual and almost linear convergence of isotherms toward the state that is characteristic for noneddy-affected zones, similar to rope 2 in the last period of observations. Current speed rapidly decreases to less than 1 cm s⁻¹.

Rope 2 (north outside the eddy) shows an increase of isotherm spacing until day 59 (28 February), probably related to the eddy moving northwest and thus more affecting this zone, followed by a stationary situation until days 66–67 (07–08 March) and then, as for the rope 1, the eddy leaves the area and its influence no longer affects the water column.

For rope 3, we observe first a stationary situation, then by day 54 (23 February), there is a strong shift in the position of

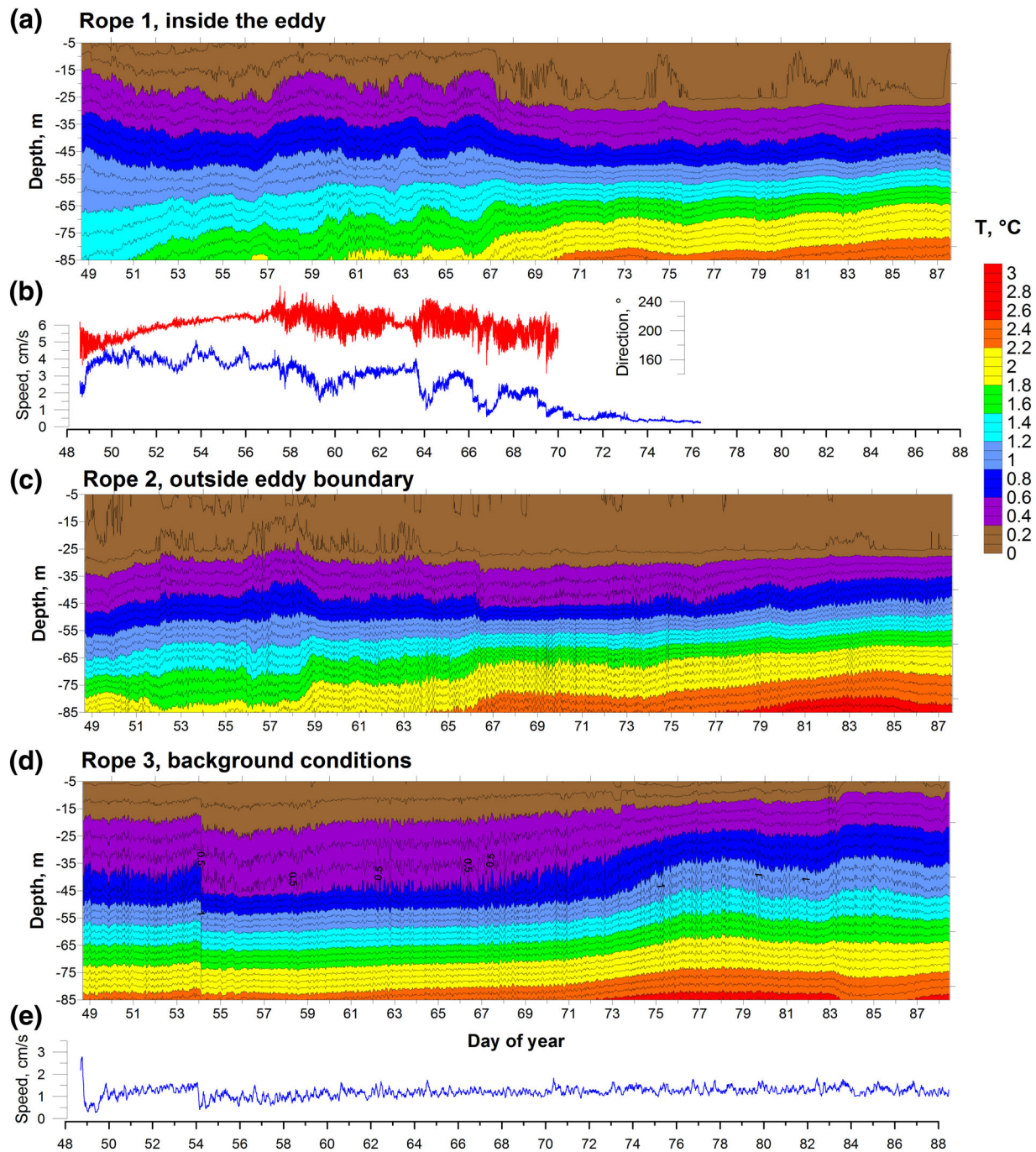


Fig. 9. Temporal evolution in February–March 2017 of the temperature profiles for the three ropes (a, c, d) and current speed and direction (not shown for weak currents as nonsignificant) for rope 1 and current speed for rope 3 (both at 45-m depth) (b, e).

the isotherms related to ice fields rafting and the vertical displacement of the rope by 4 m (to illustrate this event we did not correct depth on the figure). From this point onwards, there is a decrease in the thickness of the violet layer, probably related to convection under the ice, and the blue, blue-gray and light-blue layers rise to shallower levels and increase in thickness.

So by installing temperature sensors and current meters, we are able to analyze the influence of the eddy on the water column and precisely determine dates of spatial fluctuations and the consequent displacement of the eddy.

Despite the formation of the eddy, no ice ring appeared in 2017. This could partly be related to unusually persistent thin (up to 5–7 cm) but very dense snow cover that could have

masked surface manifestations of the melting processes. However, after the snow started to melt from 09–10 April, ice rings were still not visible. So the most evident explanation (as suggested in Kouraev et al. 2016) is that a moving eddy did not stay in the same place long enough time to melt the ice and thus to form a ring.

For all ice rings where we have observations of water structure before and during the manifestation of the ring, we may conclude that they are formed by subsurface lens-like eddies, but as 2017 observations have shown, not all eddies cause ice rings, especially when they are moving.

Discussion and conclusions

Giant ice rings in lakes

Analysis of satellite images permitted the detection of a new ice ring in 2016 and very old ones, making the total of 51 ice rings detected for Lake Baikal for 1969–2017. Corona imagery places the dates of the earliest observations of giant ice rings for Lake Baikal as 1969, again confirming that this phenomenon is not a recent one.

With the discovery of ice rings for the Teletskoye Lake, we now have three natural water bodies—lakes Baikal, Hovsgol, and Teletskoye, where these phenomena have been observed. This shows that ice rings and lens-like eddies are much more common in lakes than was known before.

All these lakes have a long narrow shape and steep bathymetry, but there is no specific reason that lens-like eddies and associated ice rings should exist only for lakes with such a shape. As long as there are conditions necessary to produce lens-like eddies, eddies could be observed by field measurements or by satellite observations. For field surveys, they will represent an anomaly of temperature and specific conductance distribution compared to surrounding waters. For satellite imagery they could be seen as ice rings, if a lake has a stable ice cover, or potentially as eddies on the open water surface—in the thermal infrared, and probably also in the visible ranges.

Temperature distribution inside the eddy

During our field work, several transects were made in February and March over the stationary eddy in 2016 and over a moving eddy in 2017. While our previous observations were limited by 100-m depth, now the temperature profiles have been made down to 160–200 m.

Based on the hypothesis of the formation of ice rings from local upwelling of the deep water, Granin et al. (2015) have applied a nonhydrostatic model and calculated the temperature field down to 400 m in the ring structure for 2009. Their results show first the deepening of the isotherms in the central part of the ring at depths between about 50 and 80 m, then rising of the isotherms at depths 130–150 m and a chimney-like inflow of warm water at depths 150–400 m. Our temperature observations do not show anything similar for depth

80–200 m. Deepening of the isotherms continues well down to 200 m and apparently below. This internal temperature structure is similar to that observed in anticyclonic lens-like eddies in the ocean, for example, in Meddies (Dugan et al. 1982; Armi and Zenk 1984; McWilliams 1985; Kostianoy and Belkin 1989; Richardson et al. 2000).

Eddy size and shape

The high spatial density of observations of water structure makes it possible to estimate the three-dimensional (3D) distribution of water properties affected by eddies. A typical eddy shape can be described as follows: a neutral layer is located at about 45–50-m depth, in the upper part, we have a dome-like rising of isotherms, that displace cold well-mixed outside water. On the lower part of the eddy, there is inclination of isotherms affecting a larger area compared to the upper dome and extending to depths of 200 m. While the ice ring size is comparable to the upper dome size, the area affected by the eddy in the neutral layer is larger (10–12 km).

Calculation of Rossby baroclinic internal radius of deformation for a two-layered fluid for our data (salinity calculated according to (Blinov et al. 2006) and density using TEOS10) gives an estimation of 1.2–1.6 km using potential density at the surface and 3.1–3.3 km using absolute density values. The ice ring external radius 3.3 km and internal radius 1.6 km are comparable with these values. The overall size of the eddy is somewhat larger than these scale length but of the same order of magnitude, suggestive of a baroclinic system close to geostrophic balance.

Currents inside the eddy and eddy rotation

Estimation of the spatial distribution of currents twice per winter was done using indirect (CTD inclination and passive drifters), and direct measurements (SeaHorse and Alec current meters). Currents are anticyclonic (clockwise direction), with low speed in the center and high speed at the eddy periphery.

The rotational speed of the eddy has been estimated from temperature variability measured at the ropes and direct current meter data between mid-February and end of March in 2016. This eddy made a complete rotation in about 3 d (radial speed 120° per day). While Meddies have much larger diameter (40–150 km), subsurface float measurements of 16 Meddies in the Atlantic (Richardson et al. 2000) show similar values for the rotational speed—their core looping period ranges between 2.5 and 6 d with an average value of 3.5 d. Continuous long-term (1.5 months) high-frequency observations of temperature (several depths) and currents (SeaHorse current meter) at various locations in the Middle Baikal also show distinct water dynamics inside and outside the eddies.

Geostrophic calculations of current speed in the eddy

Hydrographic measurements for temperature and specific conductance/salinity can be used to construct a simple layer model. If we assume that the anticyclonic ring is associated

with a lens-shaped section of uniform potential density with anticyclonic rotation, the tangential velocity on the flank of the lens can be calculated using geostrophic shallow water equations.

Since the temperature is close to the temperature of the maximum water density 4°C, the absolute values of density are not very sensitive to the temperature, so the pressure effect is significant. We have used the potential density values because the contribution of compressibility to the stratification has no influence on the baroclinic flow. Horizontal gradients of density are mostly sensitive to the temperature structure. The salinity contribution is mostly negligible—on the order of 0.025 kg m⁻³—and does not change the shape of the potential density field. Figure 10 shows the schematic potential density layer interfaces.

In the top layer above the lens, the flow velocity on the flank of the lens will be determined by the slope of the free surface, which is unknown. Within the lens, this anticyclonic flow will be strengthened by the slope of the interface. Below the lens in layer 3, the reversed slope of the interface between layers 2 and 3 is assumed to reduce this flow to zero. This assumption of nonbarotropic flow is the subject to confirmation/verification.

The expression for the flow in layer 2 within the lens is given by the equation:

$$V_2 = \frac{1}{\rho_2} \left\{ \rho_1 V_1 + \frac{g}{f} \Delta \rho |h_{1x}| \right\}$$

where V is current speed (m s⁻¹), ρ is density (kg m⁻³), g is gravity acceleration, f is the Coriolis acceleration, and h is the

thickness of the layer (m), and the flow above this in layer 1 is given by equation:

$$V_1 = \frac{g}{\rho_1 f} \Delta \rho [|h_{3x}| - |h_{1x}|].$$

We are using the values of the potential density for layers 1, 2, 3 as 999.937, 999.987, and 1000.037 kg m⁻³, respectively, using data from our field observations for February 2016. The lens is 100-m thick and the middle of the lens is located at a depth of 45 m. The gradients on the flanks of the lens cause it to close over a distance over 3.5 km. This distance represents about half of the total radius of the eddy.

The calculated value of the layer 2 velocity is 6.5 cm s⁻¹. This is slightly slower than the velocity deduced from the timing of the eddy rotation of 3 d, which for 3 km radius is 7.3 cm s⁻¹. This discrepancy could be due to ageostrophic (gradient wind balance) effects. However, the flow is close to geostrophic as indicated by a small value of the Rossby number:

$$R_a = \frac{v}{fr}$$

where v is the tangential velocity in layer 2, f is the Coriolis parameter, and r is the radius of the eddy. For the values we have calculated, this gives the Rossby number of the order of 0.1. For gradient wind balance, this would imply 10% increase in tangential velocity compared to geostrophic balance. The discrepancy between our calculations and the recorded time for one eddy revolution could also be due to an unknown barotropic component of the flow which is unknown to us since we have no measurements of the displacement of the free surface or of the deep currents.

The lifetime of the eddy can also be estimated from calculation of a damping timescale following methodology presented by Forrest et al. (2013) for an eddy observed in Pavilion Lake, British Columbia, Canada. The adjustment timescale of a rotating, stratified fluid to changes in forcing scales with the Ekman number, $E = \nu / (f * H^2)$. This represents the ratio of viscous to rotation forces, with ν the eddy viscosity and $H = 200$ m the eddy thickness (Greenspan and Howard 1963; Forrest et al. 2013). Forrest et al. (2013) used values for ν between molecular (10⁻⁶ m² s⁻¹), and 10⁻⁴ m² s⁻¹ previously reported under lake ice (Bengtsson et al. 1996). These values give E between 2*10⁻⁷ and 2*10⁻⁵. For $E \ll 1$, the adjustment time scales as $T = (E^{1/2} * f)^{-1}$. This gives a wide range of eddy lifetimes from about 20–200 d for the observed Baikal eddy. This order of magnitude calculation is consistent with some eddies lasting a few months, as seen in our satellite and in situ observations.

Traveling eddies

In 2017, an eddy appeared in February and was later found at a new position in March. The minimum speed of eddy

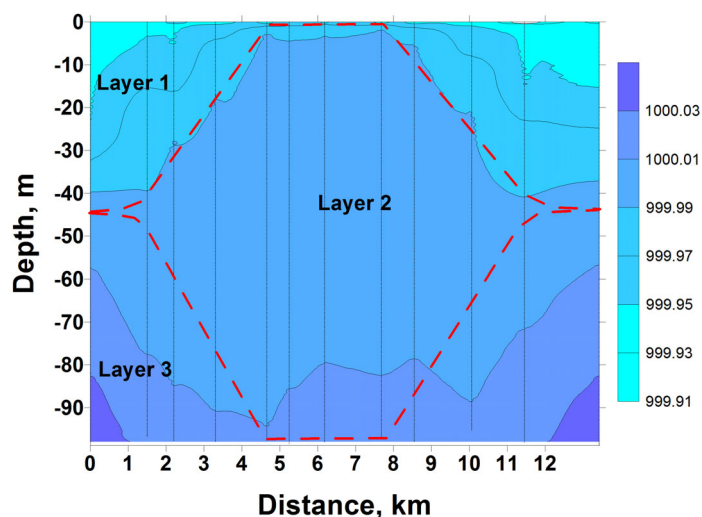


Fig. 10. Schematic layer interfaces overlaid on the vertical section of potential density (kg m⁻³) distribution across the ice ring in February 2016 (see Fig. 3 for temperature distribution). Potential density was calculated using TEOS10 equation (www.teos-10.org) basing on salinity values calculated after Blinov et al. 2006 and referenced to the surface.

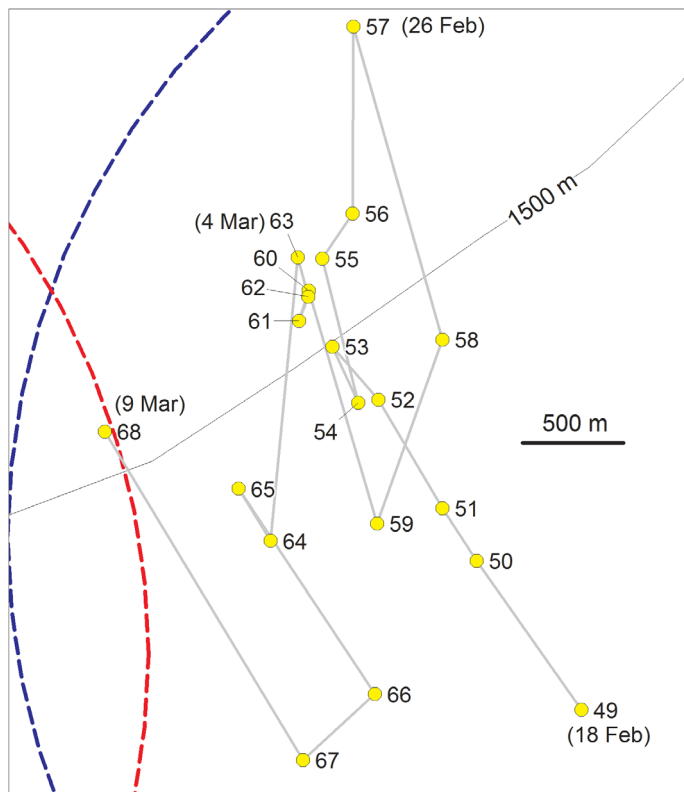


Fig. 11. Daily changes in the location of the eddy center from triangulation. Dashed circles—Approximate eddy boundaries for February (red) and March 2017 (blue), as in Fig. 7.

horizontal displacement, knowing that between mid-February and the end of March (42 d), it traveled at least 6 km, would be about 142 m d^{-1} . But as we have seen from the temperature evolution for ropes 1 and 2: (a) the eddy initially moved northwest and not directly west and (b) there were some back and forth movements of the eddy. So this estimate is a lower bound and the actual speed of eddy displacement must be greater.

To clarify this question we have tried to estimate the eddy position using temperature evolution data from ropes 1 and 2. Using data from transect across the eddy, the thickness of the layer between isotherms 0.3°C and 1.2°C (violet, blue, and gray-blue layers) was used as a proxy for distance to the eddy center. Then, using this value and comparing it to the thickness of the same layer for ropes 1 and 2, the distance to the eddy center was obtained as a function of day number for each rope. Then using triangulation, the position of the eddy center for each day was estimated (Fig. 11).

The eddy first moved northwest (days 49–57, 18–26 February), with speeds of up to 900 m d^{-1} . Then quite rapidly (1600 m d^{-1}) it started to move south-southeast toward larger depths in a clockwise movement. On days 60–63, it came back to approximately the same depths as on days 55–56. After this brief pause, the eddy made another rapid (1400 m d^{-1} between days 63 and 64) progression southwards and then (after another return to depths greater than 1500 m), it progressed clockwise toward the new location on day 68 (09 March). It appears that the eddy displayed a tendency to move toward regions with lesser depths, and this process was repeated three times. Further estimation of the eddy position is not possible as the eddy was no longer affecting the water temperature on ropes 1 and 2.

These estimates show that eddy moved in quite a complex way, with periods of stationarity followed by rapid displacements, but generally still not leaving the area with depth about 1500 m.

So far, movement of the eddies in lake Baikal was just a hypothesis. We now have documented for the first time a real case of a moving eddy, with estimation of timing of movement, location of the eddy center, and speed of eddy displacement between mid-February and end of March in 2017. The speed of eddy displacement (up to $1400\text{--}1600 \text{ m d}^{-1}$, or $1.6\text{--}1.85 \text{ cm s}^{-1}$) corresponds well to the background current speed ($1.5\text{--}2 \text{ cm s}^{-1}$) at these depths (see also Fig. 9e).

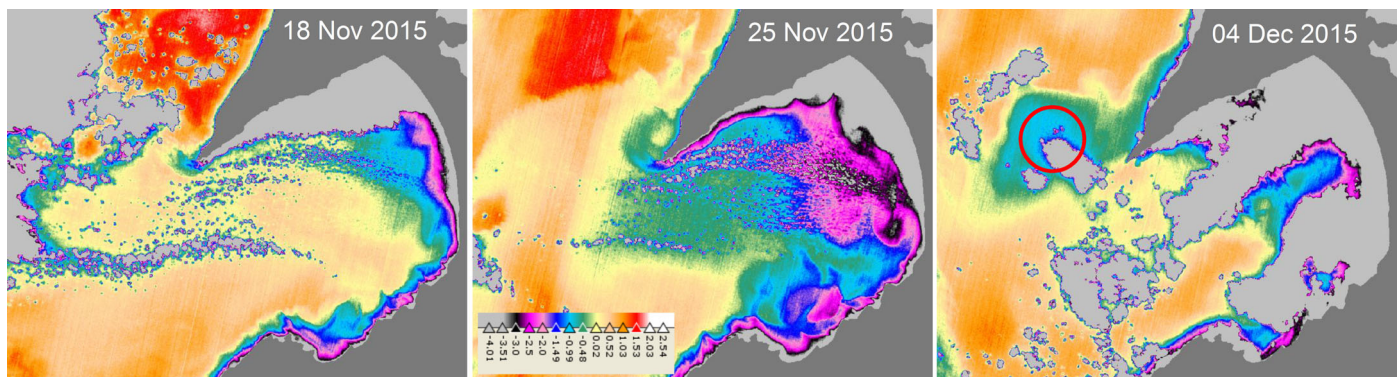


Fig. 12. Surface temperature. Landsat 8, thermal infrared band 10, temperature calculated using coefficients from (Landsat 8 product web site, 2018). Light gray color—Clouds, dark gray—Land mask. Red circle on the image from 04 December 2015—Location of the ice ring as defined on 01 April 2016.

Mechanism of eddy formation

Detection of eddies in February 2016 and 2017 not long after the formation of stable ice cover suggests that they probably do not develop under ice cover, but are generated at some time between autumnal overturning and ice cover formation, and are potentially related to the influence of the wind on the ice-free water surface.

In the case of the eddy observed in 2016, we may estimate its generation and development using satellite thermal imagery in November and December 2015. According to the 3-hourly in situ data on wind speed and direction at the Ust-Barguzin meteorological station, during November–December 2015, there was a constant $2.5\text{--}3\text{ m s}^{-1}$ wind from the east–southeast (57.8%) or southeast (11.1%) directions. This wind was moving large volume of water from the shallower and thus colder Barguzin Bay to the open part of Lake Baikal. This movement may be estimated from a temporal sequence of thermal imagery from the Landsat 8 satellite (Fig. 12).

On the 18 November, the coldest water is observed along the shallow regions of the Barguzin Bay. In the region of the Nizhneye Izgolovye Cape (the Svyatoy Nos Peninsula acts as a wall blocking the outflow), there is a plume of colder ($0.5\text{--}1.3^{\circ}\text{C}$) and thus lighter (as its temperature is below 3.98°C) water in the still warm ($2.2\text{--}2.8^{\circ}\text{C}$) central part of the lake. On the 25 November, a large part of the Barguzin Bay is occupied by cold water and near the Nizhneye Izgolovye Cape, the outflow defined earlier now starts to form an anticyclonic eddy. On the 04 December, this eddy is well formed and has detached itself from the coast, located about 10 km from the cape, over the head of the underwater depression with depth 1500 m and more. The position of its core ($0.3\text{--}0.6^{\circ}\text{C}$) is in perfect agreement with the position of the future eddy and ice ring as defined in February–April 2016.

So we now have evidence that an eddy was formed in 2016 by outflow of water from the Barguzin Bay and that in this case the main driver of eddy generation is the wind-induced movement of colder and lighter water in association with the coastline shape. We suggested this mechanism in our previous publication where we presented satellite images of anticyclonic eddies formation in the same region in the autumn 2011 and 2014 (Kouraev et al. 2016, 2018).

Granin et al. (2015) have analyzed heat fluxes in the ice cover and in the system water–ice. They calculated variations in the ice thickness inside the ring in Southern Baikal in 2009 in the framework of the Stefan problem using a two-dimensional axis-symmetrical model and current speed from a 3D nonhydrostatic model (using the upwelling of deep water hypothesis). They estimate the period of ring formation as 25 to 35 d. This would mean that for this ice ring, that appeared in early April 2009, the generation of currents below the ice (that led to formation of ice ring) should have happened in late February–early March 2009 (stable ice cover was formed on 23 January).

It is not possible to estimate the driving force of eddy generation without in situ data before the formation of the ice ring in Southern Baikal in 2009 or near Cape Krestovskiy in 2013. However, for the region of the Nizhneye Izgolovye Cape, there are several cases that appear to contradict the hypothesis of upwelling of deep water (Granin et al. 2018) and the results of estimation of period for the formation of the ring structure (Granin et al. 2015).

For example, in the region of Nizhneye Izgolovye Cape in 2009 (Kouraev et al. 2016) stable ice cover was formed on 13 January and the ice ring was already visible 18 d later (01 February), so the eddy must have been formed before ice formation. Moreover, the sequence of thermal images showing eddy formation in November–December 2015 (Fig. 12) shows that (a) the eddy was generated by the wind and (b) the time between eddy formation (approximately end of November 2015) and the first observation of the ice ring (16 March 2016) indicates a much longer time (about 3.5 months).

Further research

Processes under ice have usually been considered as less important and on a much smaller scale compared to the ice-free period, but this view is changing. There is a recent increase in the number of scientific publications addressing physical, chemical, and biological processes under ice cover (Powers and Hampton 2016). Our results show that the upper 0–200 m layer below the ice cover does not represent a “static landscape” with the well-mixed upper layer and stratified lower layer that are gradually affected by vertical convection in the spring. Throughout the winter, there are also high-energy processes of water exchange related to quasi-stationary or moving intrathermocline eddies.

Lakes with stable (no ice drift) ice cover represent a perfect opportunity to study such lens-like eddies using in situ observations as compared to the oceans or seas. Since such eddies in the ocean are moving, ship observations usually provide just several transects over the eddies, and mooring stations may just reveal the passage of the eddy across these stations. Also, detection of lens-like eddies in the ocean is quite often a question of chance.

In the case of Lake Baikal, where eddies are either stationary or moving (but not over long distances), and where we know the locations of frequent eddy occurrence, work from ice and installation of chains with instruments anchored in the ice provide a unique opportunity for continuous long-term monitoring of these phenomena.

Further studies of water dynamics (before ice formation and during ice cover presence) from satellite imagery, field observations and autonomous loggers, as well as numerical and laboratory modeling, will hopefully bring new insights to help understand and monitor complex dynamical processes taking place in winter time. This includes the generation and evolution of lens-like eddies and giant ice rings (as their

surface manifestations) not only in lakes Baikal, Hovsgol and Teletskoye, but possibly in other lakes of the world.

References

- Armi, L., and W. Zenk. 1984. Large lenses of highly saline Mediterranean water. *J. Phys. Oceanogr.* **14**: 1560–1576.
- Bengtsson, L., J. Malm, A. Terzhevik, M. Petrov, P. Boyarinov, A. Glinisky, and N. Palshin. 1996. Field investigation of winter thermo- and hydrodynamics in a small Karelian lake. *Limnol. Oceanogr.* **41**: 1502–1513. doi:<https://doi.org/10.4319/lo.1996.41.7.1502>
- Blinov, V. V., N. G. Granin, R. Y. Gnatovskii, A. A. Zhdanov, and S. Rimkus. 2006. Determining water masses in Lake Baikal by T,S-analysis. *Geogr. Nat. Res.* **2**: 63–69 (In Russian).
- Dugan, J. P., R. R. Mied, P. C. Mignerey, and A. F. Schuetz. 1982. Compact, intrathermocline eddies in the Sargasso Sea. *J. Geophys. Res.* **87**: 385–393.
- Forrest, A. L., B. E. Laval, R. Pieters, and D. S. S. Lim. 2013. A cyclonic gyre in an ice-covered lake. *Limnol. Oceanogr.* **58**, 2013: 363–375. doi:[10.4319/lo.2013.58.1.0363](https://doi.org/10.4319/lo.2013.58.1.0363)
- Galaziy, G. I. [ed.]. 1993. *Baikal Atlas*. (In Russian, Russian Academy of Sciences, Siberian branch). Moscow: Federal Service of Geodesy and Cartography.
- Granin, N. G., and others. 1999. Turbulent mixing in the water layer just below the ice and its role in development of diatomic algae in Lake Baikal. *Doklady Akademii Nauk.* **366**: 835–839, in Russian.
- Granin, N. G., Wüest, A., Gnatovskii, R. Y., and Kapitanov, V. V. 2005. Evidence of activity of mud volcanoes in Baikal, in: *The Fourth Vereshchagin Baikal Conference: Abstracts of Papers and Posters*, 26 September–1 October, 2005 [in Russian]. Institute of Geography SB RAS, Irkutsk, pp. 52–53.
- Granin N.G, Makarov, M.M., Kucher, K.M., & Gnatovsky, R.Y. 2008. The deep water gas seeps in Lake Baikal. *Proceedings of the 9th International Conference on gas in marine sediments*, Bremen, Germany, 15–19 September, p. 76–77.
- Granin, N. G., V. V. Kozlov, E. A. Tsvetova, and R. Y. Gnatovsky. 2015. Field studies and some results of numerical modeling of a ring structure on Baikal ice. *Doklady Earth Sci.* **461**: 316–320.
- Granin, N. G., and others. 2018. Natural ring structures on the Baikal ice cover: Analysis of experimental data and mathematical modeling. *Russian Geol. Geophys.* **59**: 1514–1525. doi:<https://doi.org/10.1016/j.rgg.2018.10.011>
- Graves K. E. 2015. Under-ice circulation in an Arctic Lake: Observations from two field seasons in Lake Kilpisjarvi, Finland. Master thesis, The Faculty of Graduate and Postdoctoral Studies (Civil Engineering), The Univ. of British Columbia. Vancouver, 69 p.
- Greenspan, H. P., and L. N. Howard. 1963. On a time-dependent motion of a rotating fluid. *J. Fluid Mech.* **17**: 385–404.
- Heim, B., H. Oberhaensli, S. Fietz, and H. Kaufmann. 2005. Variation in Lake Baikal's phytoplankton distribution and fluvial input assessed by SeaWiFS satellite data. *Glob. Planet Ch.* **46**: 9–27.
- Kirillin, G. B., A. L. Forrest, K. E. Graves, A. Fischer, C. Engelhardt, and B. E. Laval. 2015. Axisymmetric circulation driven by marginal heating in ice-covered lakes. *Geophys. Res. Lett.* **42**: 2893–2900.
- Kostianoy, A. G., and I. M. Belkin. 1989. A survey of observations on intrathermocline eddies in the World Ocean. In: *Proceedings of 20-th international liege colloquium ocean hydrodyn*, p. 821–841. In J. C. J. Nihoul and B. M. Jamart [eds.], *Mesoscale/synoptic coherent structures in geophysical turbulence*. Amsterdam: Elsevier.
- Kouraev, A. V., S. V. Semovski, M. N. Shimaraev, N. M. Mognard, B. Legresy, and F. Remy. 2007a. Observations of lake Baikal ice from satellite altimetry and radiometry. *Rem. Sens. Environ.* **108**: 240–253.
- Kouraev, A. V., S. V. Semovski, M. N. Shimaraev, N. M. Mognard, B. Legresy, and F. Remy. 2007b. Ice regime of lake Baikal from historical and satellite data: Influence of thermal and dynamic factors. *Limnol. Oceanogr.* **52**: 1268–1286.
- Kouraev, A. V., Zakharova E. A., Rémy F., Suknev A.Ya. 2015. Study of Lake Baikal ice cover from radar altimetry and in situ observations. *Marine Geodesy* **38**: 477–486. <https://doi.org/10.1080/01490419.2015.1008155>
- Kouraev, A. V., E. A. Zakharova, F. Rémy, A. G. Kostianoy, M. N. Shimaraev, N. M. J. Hall, and S. A. Ya. 2016. Giant ice rings on Lakes Baikal and Hovsgol: Inventory, associated water structure and potential formation mechanism. *Limnol. Oceanogr.* **61**: 1001–1014. doi:[10.1002/lno.10268](https://doi.org/10.1002/lno.10268)
- Kouraev, A. V., E. A. Zakharova, N. N. Filatov, S. Baklagin, K. Barbieux, B. Merminod, D. V. Pozdnyakov, and D. A. Kondrik. 2017. Multiscale multispectral remote sensing of ice cover in lakes Onego and Ladoga using a combination of spaceborne, aerial drone and ground-based measurements. In: *Proceedings of the 1st international conference "Lakes of Eurasia: Problems and solutions"*, September 11–15, Petrozavodsk, Russia.
- Kouraev, A. V., E. A. Zakharova, F. Rémy, M. N. Shimaraev, A. G. Kostianoy, and A. Y. Suknev. 2018a. Ice cover of Eurasian lakes from satellite and in situ observations. In: *Proceedings of the international conference, "Freshwater ecosystems - key problems"*, September 10–14, Irkutsk, Russia.
- Kouraev, A. V., E. A. Zakharova, F. Rémy, A. G. Kostianoy, M. N. Shimaraev, N. M. J. Hall, and A. Suknev. 2018b. Ya. Ice cover and water dynamics in lakes Baikal and Hovsgol from satellite observations and field studies, p. 541–555. In S. Vignudelli and M. Gade [eds.], *Remote sensing of Asian seas*. Springer.
- Kouraev, A. V., E. A. Zakharova, F. Rémy, A. G. Kostianoy, M. N. Shimaraev, N. M. J. Hall, R. E. Zdorovenov, and

- S. A. Ya. 2018c. Giant ice rings on lakes Baikal and Tel-etskoeye and field observations of lens-like eddies in the Middle Baikal (2016b–2017). In: *Proceedings of the ASLO summer meeting*, 10–15 June 2018, Victoria, BC, Canada.
- Kouraev A. V., Zakharova E. A., Rémy F., Shimaraev M.N., Kostianoy A. G., and A. Y. Suknev. (2018d). Ice cover of Eurasian lakes from satellite and in situ observations. *Proceedings of the international symposium "25 years of progress in radar altimetry"*, 24–29 September 2018, Ponta Delgada, Portugal.
- Landsat 8 web site. 2018. [accessed 2018 March 20]. Available from <https://landsat.usgs.gov/using-usgs-landsat-8-product>
- Lawrence, S. P., K. Hogeboom, and H. L. L. Core. 2002. A three-dimensional general circulation model of the surface layers of Lake Baikal. *Hydrobiologia* **487**: 95. doi:<https://doi.org/10.1023/A:1022938009360>
- Le Core Helen Louise. (1998). Use of numerical models and satellite data to study physical processes in Lake Baikal. Thesis submitted for the degree of Doctor of Philosophy at the Univ. of Leicester. Leicester, 136 p.
- Leech, D. M. 2018. Satellites and sensors tell us more about the Giant Ice Rings of Siberian Lakes. *Limnol. Oceanogr. Bull.* **27**: 119–120. doi:<https://doi.org/10.1002/lob.10278>
- Mackay, A. W., R. W. Battarbee, R. J. Flower, N. G. Granin, D. H. Jewson, D. B. Ryves, and M. Sturm. 2003. Assessing the potential for developing internal diatom-based inference models in Lake Baikal. *Limnol. Oceanogr.* **48**: 1183–1192.
- Mackay, A. W., D. B. Ryves, R. W. Battarbee, R. J. Flower, D. Jewson, P. Rioual, and M. Sturm. 2005. 1000 years of climate variability in Central Asia: Assessing the evidence using Lake Baikal diatom assemblages and the application of a diatom-inferred model of snow thickness. *Glob. Planet. Ch.* **46**: 281–297.
- McWilliams, J. C. 1985. Submesoscale, coherent vortices in the ocean. *Rev. Geophys.* **23**: 165–182.
- Mitrofanova, E. Y., and V. V. Kirillov [eds.]. 2012. Lake Tel-etskoeye, Institute of water and ecological problems SB RAS Publishing, v. **28**. Novosibirsk.
- Moore, M. V., S. E. Hampton, L. R. Izmet'seva, E. A. Silow, E. V. Peshkova, and B. Pavlov. 2009. Climate change and the world's "Sacred Sea"—Lake Baikal, Siberia. *Bioscience* **59**: 405–417.
- Powers, S. M., and S. E. Hampton. 2016. Winter limnology as a new frontier. *Limnol. Oceanogr.* **25**: 103–108.
- Richardson, P. L., A. S. Bower, and W. Zenk. 2000. A census of Meddies tracked by floats. *Oceanogr.* **45**: 209–250. doi:[https://doi.org/10.1016/S0079-6611\(99\)00053-1](https://doi.org/10.1016/S0079-6611(99)00053-1)
- Semovski, S. V., N. Y. Mogilev, and P. P. Sherstyankin. 2000a. Lake Baikal ice: Analysis of AVHRR imagery and simulation of under-ice phytoplankton bloom. *J. Mar. Syst.* **27**: 117–130.
- Semovski, S., N. Mogilev, N. Minko, E. Loupian, and A. Mazurov. 2000b. Fusion of data sources in an effort to study global climate change for the great lakes of north Eurasia. *Int. Arch. Photogramm. Remote Sens.* **33**: 925–930.
- Troitskaya, E., V. Blinov, V. Ivanov, A. Zhdanov, R. Gnatovsky, E. Sutyryna, and M. Shimaraev. 2015. Cyclonic circulation and upwelling in Lake Baikal. *Aquat. Sci.* **77**: 171–182. doi:<https://doi.org/10.1007/s00027-014-0361-8>
- Tsvetova, E. A. 1999. Mathematical modelling of Lake Baikal hydrodynamics. *Hydrobiologia* **407**: 37. doi:<https://doi.org/10.1023/A:1003766220781>
- Verbolov, V. I., V. M. Sokol'nikov, and M. N. Shimaraev. 1965. Hydrometeorological regime and heat balance of Lake Baikal. (Gidrometeorologicheskiiy regim i teplovoy balans oz. Baikal, in Russian). (Moscow-Leningrad. "Nauka").

Acknowledgments

This research was supported by the ERA.NET RUS Plus S&T #226 "ERALECC," CNES TOSCA "Lakelce," RFBR 19-05-00522, RFBR-RGO 17-05-41043, CNRS PICS "BaLaLaCA," Toulouse Arctic Initiative, RFBR 13-05-91051, GDRI "Car-Wet-Sib," IRN TTS and IDEX InHERA projects. Corona and Landsat data are available from the U.S. Geological Survey. A.G. Kostianoy was partially supported in the framework of the P.P. Shirshov Institute of Oceanology RAS (Russian Academy of Sciences) budgetary financing (Project N 0149-2019-0004). We would like to thank A. Beketov and M. Fomenko (Ust' Barguzin, Russia), M. Ovdin and N. Makoveev ("Zapovednoye Podlemorye," Ust' Barguzin, Russia), P. Zavyalov and A. Osadchiv (Shirshov Institute of Oceanology RAS, Moscow), S. Sushkeev (Tunka Regional Administration, Russia), Hurga and Byamba (Hovsgol National Park, Mongolia), A. Laletin (Krasnoyarsk), and many others who participated directly or helped to organize field surveys. We would like to thank N. Palshin (Northern Water Problems Institute, Karelian Center of RAS, Petrozavodsk, Russia), V. Zyryanov (Institute of Water Problems RAS, Moscow, Russia), and many other colleagues for interesting and helpful discussions.

Conflict of interest

None declared.

Submitted 11 May 2018

Revised 11 December 2018

Accepted 26 August 2019

Associate editor: Sally MacIntyre